Defence Science Journal, Vol. 63, No. 2, March 2013, pp. 164-173, DOI: 10.14429/dsj.63.4259

RESEARCH PAPER

Flight Test Evaluation of Mission Computer Algorithms for a Modern Trainer Aircraft

Gargi Meharu, Sunil K. Valsan, and Rajesh A. Kuttieri*

Hindustan Aeronautics Limited, ARDC, Bangalore-560 037, India
**E-mail: sm.av.ardc@hal-india.com*

ABSTRACT

A low cost integrated avionics system has been realized on a modern trainer aircraft. Without using an expensive inertial navigation system onboard, acceptable level of accuracy for navigation, guidance, and weapon aiming is achieved by extensive data fusion within mission computer. The flight test evaluation of mission computer is carried out by assessing the overall performance under various navigation and guidance modes. In flight simulation is carried out for weapon aiming modes. The mission computer interfaces with various subsystems and implements the functional requirements for flight management and mission management. The aim of this paper is to discuss the algorithms of a data fusion intensive mission computer and flight test evaluation of these algorithms, for a typical modern trainer aircraft. The challenges and innovations involved in the work are also discussed.

Keywords: Mission computer, head-up-display, navigation and guidance algorithms

NOMENCLATURE

$(x1,y1)$	Present Position
$(x2,y2)$	Targeted Position
λ_1	Latitude of point $(x1, y1)$
λ_2	Latitude of point $(x2, y2)$
λ_p	Latitude of present position
λ_d	Latitude of destination
μ_1	Longitude of point $(x1, y1)$
μ_2	Longitude of point $(x2, y2)$
μ_p	Longitude of present position
μ_d	Longitude of destination
R	Mean radius of earth
Ψ	True heading
χ	Track angle
ξ	Drift angle
χ_D	Desired Track (deg)
χ_n	Course of nth leg of FPL
χ_L	Inverse of course of current FPL leg
χ_H	Bearing of $(x2, y2)$ from $(x1, y1)$
χ_P	Bearing of $(x1, y1)$ from $(x2, y2)$
r_H	Range of $(x2, y2)$ from $(x1, y1)$
r_D	Track component of r_H
V	True air speed
V_c	Calibrated air speed
V_g	Ground speed
V_n	Inertial velocity - North
V_e	Inertial velocity – East
V_{an}	Air speed - North
V_{ae}	Air speed – East
R_x	Range to DEST -ground axis (N)
R_y	Range to DEST -ground axis (E)
R_z	Range to DEST -ground axis (D)
R_i	Range to DEST -aircraft axis (i)
R_j	Range to DEST -aircraft axis (j)
R_k	Range to DEST -aircraft axis (k)
σ	Air density ratio
u	Factor in steering error computation
d	Cross track deviation
H_R	Filtered radio height
H_B	Barometric altitude
H_D	Elevation of the destination point
X	x distance between two points
Y	y distance between two points
Z	z distance between two points
X_c	Azimuth of 'close nav cross'
Y_c	Depression of 'close nav cross'
W_n	wind vector-North
W_e	wind vector-East

1. INTRODUCTION

A mission computer (MC) which interfaces with various subsystems and implements the functional requirements for flight management and mission management is generally considered as the avionics central computer of a military aircraft. Based on the operational and maintenance philosophy and the intended platform, the architecture, functional aspects, and criticality of MC may vary. A low cost integrated avionics system is realized for a modern trainer aircraft around a MC with set of cockpit displays and subsystems like air data system (ADS), global positioning system (GPS), attitude and heading reference system (AHRS), angle of attack probe (AOA), and radio altimeter (RADALT)[1]. The term low cost is used considering the fact that the integrated avionics architecture does not include the expensive inertial navigation system onboard and the acceptable level of accuracy for navigation, guidance, and weapon aiming is realized with the extensive

Received 17 September 2012, revised 08 February 2013, online published 23 March 2013

data fusion within the MC. The MC drives the cockpit displays like Head-up-display (HUD) and HUD repeater to aid the pilots to perform basic flight management, navigation and guidance, and weapon aiming. The MC discussed in this paper is based on Power PC processor and it is realized with open architecture concept to certain extent.

The MC is networked with other subsystems primarily on ARINC-429 data bus and video interfaces. The interfaces of MC with the other systems are shown in Fig 1. The HUD camera captures the HUD symbology and outside world imagery and this combined video is made available on HUD Repeater and for video recording system (VRS) with necessary synthetic symbologies superimposed by MC. The onboard data recorder and differential GPS, both part of flight test instrumentation (FTI), are also shown in Fig. 1.

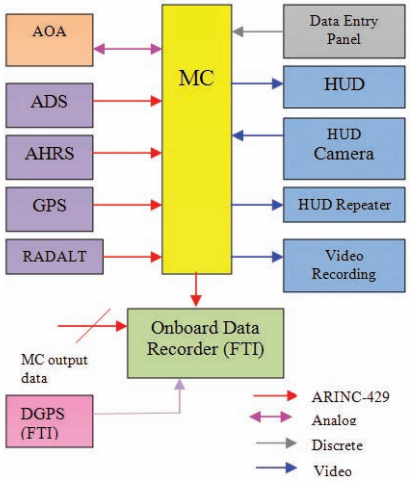

Figure 1. Integrated avionics architecture.

The MC algorithms and flight test evaluation of navigation and guidance algorithms are discussed in this paper. The navigation algorithm of MC uses extended data fusion of GPS, AHRS, ADC, and AOA parameters. The GPS is updated at low update rate, typically at 1 Hz. The MC algorithm predicts the smoothened navigation coordinates by data fusion of GPS and AHRS parameters; and corrects with the fresh GPS data using appropriate digital filter. The wind vector is estimated by the MC by using true air speed from ADC and ground speed from GPS. In the case of invalid GPS data, the MC uses ADC data for dead reckoning mode navigation along with the previously computed wind vector. The required axis transformations are processed by MC using AOA, attitude, and heading data. For low altitude up to 1500 m above ground, the radio height is considered and the raw data from RADALT is processed through a digital filter for smoothened indication in the cockpit and for computations. The MC performs the processing of data from different subsystems, analysis and annunciates health status of individual subsystems, generates stall warning and ground proximity warning, drives the cues on HUD for navigation, guidance, flight and mission management, Discrete and pre-flight mission data loading. The MC is also embedded with algorithms for weapon aiming for air to ground and air to air modes.

The various guidance modes in the MC are; manual waypoint navigation, manual flight plan navigation, auto flight plan navigation, time navigation, close navigation, and dead reckoned navigation. The close navigation is done in baro ranging or radio ranging or vertical velocity filter mode, based on the validity of the input data to the MC. The dead reckoned mode is activated while GPS data is interpreted as invalid.

The lateral guidance modes in the MC are classified as direct to fix (DTF) and course to fix (CTF), generally for the manual navigation and auto navigation respectively. In the auto navigation, the guidance mode will be DTF till the first leg (of flight plan) destination is approached (either in terms of steering error or in terms of time to go), and then the mode will be switched to CTF till the navigation is completed in the active flight plan. In manual navigation, DTF is commonly used. The various guidance cues displayed on HUD include bearing, range, present position coordinates, destination index or waypoint number, steering pointer, steering index, track index, drift angle, heading, close navigation cross, time to go, expected time of arrival, NTR circle, desired calibrated air speed, and cross track deviation.

For the flight testing and the post-flight analysis of the navigation and guidance algorithms, the flight test instrumentation (FTI) consisting of telemetry and onboard recorded flight data, audio, and HUD video were referenced. Apart from the aircraft GPS, a differential GPS (DGPS-post processed) data as part of FTI was used as the bench mark for the accuracy of the MC computed navigation coordinates. The MC algorithm was simulated in offline and stimulated using the sensor data recorded during flight. The MC simulation output, in-flight recorded HUD video, mission plan, test pilots feedback, telemetry observations, and flight data recorded from ADC, AHRS, GPS,RADALT, MC, and FTI-DGPS were utilized for the post flight analysis. A closed flight trajectory, similar to a box pattern, was carried out for flight evaluation of MC navigation and guidance algorithms. Implementation of the MC algorithms and flight test evaluation of navigation and guidance algorithms are elaborated in the following sections.

The weapon aiming simulation has been carried out in flight under air to air and air to ground attack modes. The air to ground mode includes – fixed mode, gyro stabilised mode, and CCIP mode. The AA modes include – lead angle computation (LAC) mode and CCIL mode. For the sake of completeness, the simulated checks (in-flight) of weapon aiming algorithms are also discussed in following sections.

2. NAVIGATION AND GUIDANCE ALGORITHMS

The navigation and guidance algorithms embedded in MC are described in this section. The necessary checks to avoid singularity cases and range limits are appropriately implemented. The spherical earth model is assumed in computing great circle bearing and range. The velocity components in geographical axes are complementary filtered by MC using ground speed components derived from GPS data and acceleration components in geographical axes derived from AHRS data. The present position coordinates are smoothened using previous coordinates and filtered ground speed components in geographical axes. This prediction is corrected whenever fresh valid GPS data is received[2,3].

The various computations are discussed in the following paragraphs. The conventions used in the following equation are; λ is latitude, μ is longitude, R is mean radius of earth, V_g is ground speed, V_n and V_e are velocity components, and W_n and W_e are wind velocity components.

Complementary filtering for PP under valid GPS data and wind vector estimation

$V_n = V_n + An*dt$
$V_e = V_e + A_{e*} dt$
$\lambda_p = \lambda p + V_n *dt/R$
$\mu_p = \mu_p + V_e*dt /R (\cos \lambda_p)$
If (GPS_NEW)
$V_n = V_n + (V_{GPS} * \cos(\chi_{GPS}) - V_n) /t_1$
$V_e = V_e + (V_{GPS} * \sin(\chi_{GPS}) - V_e)/t_1$
$\lambda_p = \lambda_p + (\lambda_{GPS} - \lambda p) / t_2$
$\mu_p = \mu_p + (\mu_{GPS} - \mu p) / t_2$
End If.

The wind vectors are estimated using the true air speed resolved into geographical axes and ground speed resolved into geographical axes, and then using the appropriate digital filter.

$V_{an} = V * (L_{11}*\cos(\alpha)+N_{11}*\sin(\alpha))$
$V_{ae} = V *(L_{21}*\cos(\alpha)+N_{21}*\sin(\alpha))$
$W_n = W_n +(dt/t_3)*(V_n-V_{an}-W_n)$
$W_e = W_e +(dt/t_3)*(V_e-V_{ae}-W_e)$

Here, L_{11}, N_{11}, L_{21}, and N_{21} are directional cosine matrix coefficients. The parameter dt is the refresh time period; and t_1, t_2, and t_3 are time constants of navigation filters.

Bearing, range and time to go computations

$X = (\cos \lambda_1 * \sin \lambda_2) – (\sin \lambda_1 * \cos \lambda_2 * \cos (\mu_2 - \mu_1))$
$Y = \cos \lambda_2 * \sin (\mu_2 - \mu_1)$
$Z = \sin \lambda_1 *\sin \lambda_2 +\cos \lambda_1 *\cos \lambda_2 * \cos (\mu_2 - \mu_1))$
$\chi_H = \text{atan2}(Y, X)$
$r_H = R * \text{atan2} (\text{sqrt}(X^2+Y^2), Z)$
$t_{go} = r_{H / Vg}$

Track, drift angle and ground speed computations

$\chi = \text{atan2} (V_e, V_n)$
$\xi = \chi – \psi$
$V_g = {}_{Sqrt}(V_n{}^{2} + V_e{}^{2})$

Cross track deviation and desired track computation

If (Guidance Mode is ‘DTF’)
$\chi_D = \chi_H$
$\chi_L = \chi_P$
Else If (Guidance Mode is ‘CTF’)
$\chi_L = \chi_{n-\Pi}$
$\chi_D = \text{atan2} (-\cos \lambda_d * \sin \chi_L ,(\sin(r_D / R) *\sin\lambda_d) –(\cos(r_D/ R)*\cos \lambda_d *\cos \chi_L))$
End If
$r_D = r_H * \cos (\chi_L - \chi_P)$
$d = r_H * \sin (\chi_L - \chi_P)$
$u = d/(t * Vg)$

Steering error computation

If (Guidance mode is ‘DTF’)
Steering error = $\chi_D - \chi$
Else If (Guidance mode is ‘Course To Fix’)
Steering Error = $\chi_D - \chi - u$
End If

Dead reckoned mode navigation

$V_n = V_{an} + W_n$
$V_e = V_{ae} + W_e$
$\lambda_p = \lambda p + V_n *dt/R$
$\mu_p = \mu_p + V_e*dt /R (\cos \lambda_p)$

Close navigation computation

$R_x = r_{H*} \cos (\chi_H - \psi)$
$R_y = r_{H*} \sin (\chi_H - \psi)$
$R_z = H_{R\ 'OR'}\ R_z = H_B - H_D$
$R_i = [DCM] [R_x, R_z]$
$R_j = [DCM] [R_x, R_y, R_z]$
$R_k = [DCM] [R_x, R_y, R_z]$
$X_c = R_j / R_i$
$Y_c = R_k / R_i$

Time navigation

Compute a value of destination time that is compensated for the 12 am discontinuity (if necessary). Here,‘t’ is current time, ‘tdest’ is destination time, and ‘T_d’ is destination time compensated for 12 am discontinuity.

If (t – tdest > 43200) then
T_d = tdest + 86400)
Else
T_d = tdest
End if

Adjustment for flight delay by Delay_Time (negative delay indicates early take-off)

If (Delay_Time > 0)
$T_d = T_d$ + Delay_Time
Else
$T_d = T_d$ – Delay_Time
End If
If (TNAV and tdest.Validity = “True” and $t < T_d$) then
If (NEW_DEST or ($r_H > 5000$ and [Td – t] > 10)) then
If ($T_d – t > 10$)
$V_D = r_H / (T_d – t)$
Else
$V_D = r_H / 10$
End if
$(V_c)_D = V_c + (V_D – V_g) \sqrt{\sigma}$
Limit $(V_c)_D$
Else
$(V_c)_D$ frozen at previously computed value
End if
Else
$(V_c)_D$ .Validity = “False”
End if.

3. FLIGHT TEST EVALUATION

A closed flight trajectory similar to a box pattern with seven destination points was carryout for the flight evaluation of MC navigation and guidance algorithms. For the purpose of flight testing, an accurate post processed DGPS (part of flight test instrumentation) was taken as the master reference for navigation parameters. Proper time synchronization for the data recorded from various sources was ensured during post

processing. For the performance analysis discussed in this paper, the different data set such as onboard recorded avionics bus data, post processed FTI-DGPS data, and audio and video recorded by VRS were utilized. The direct navigation, planned track navigation, time navigation, auto/ manual navigation, and close navigation functionalities have been flight tested. The quantitative analysis was carried out by an MC algorithm simulation tool, stimulated with the flight data. The analysis plots are generated using this tool. Following sections describe the quantitative and qualitative analysis.

Case A: Auto Navigation

The flight plan (FPL) was created and activated under auto navigation mode. The FPL is shown in Table 1 and Fig. 2 as two dimensional presentations.

Table 1. Flight plan (FPL) presentation

DEST No. of FPL	WPT No.	Way point details	
		Latitude (deg min)	Longitude (deg min)
01	001	12 57.1	77 40.2
02	002	12 43.4	77 50.4
03	004	12 39.5	78 01.2
04	008	12 28.5	78 11.2
05	009	12 47.9	78 16.6
06	010	13 11.2	78 09.9
07	001	12 57.1	77 40.2

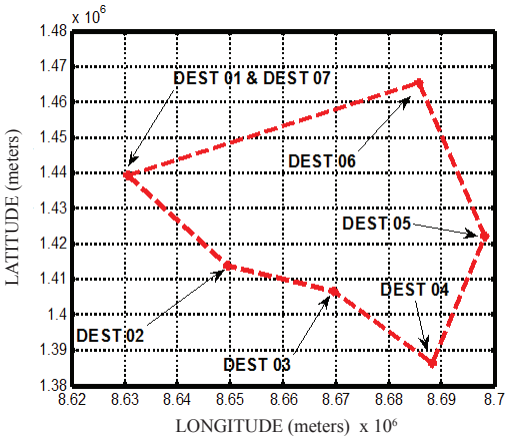

Figure 2. FPL Profile, planned trajectory.

The planned path of the flight trajectory is shown in Fig. 2 and the actual path followed by the aircraft with respect to the planned path is shown in Fig. 3. The computed bearing and range for each leg of the FPL is shown in Table 2. Figures 4 to 6 show the trajectory of different legs of the FPL.

Under auto navigation mode, the direct to fix method provides horizontal guidance to reach to the point along a straight line connecting the present position and the desired waypoint. The course to fix guidance provides the guidance to reach the desired waypoint along a pre-determined track.The guidance mode is in DTF initially for leg-01 till the steering error is less than 5 degrees. Once the mode is switched to CTF,

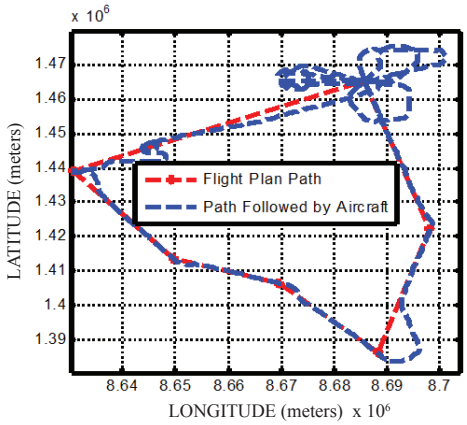

Figure 3. Actual track overlayed with FPL.

Table 2. Computed bearing and range for FPL legs.

FPL leg	MC computed bearing and range using MC algorithm simulation tool	
	Bearing (deg) from aircraft to destination	Range (km)
01	140.99	31.97
02	110.11	11.28
03	138.79	4.679
04	14.89	16.888
05	344.46	20.21

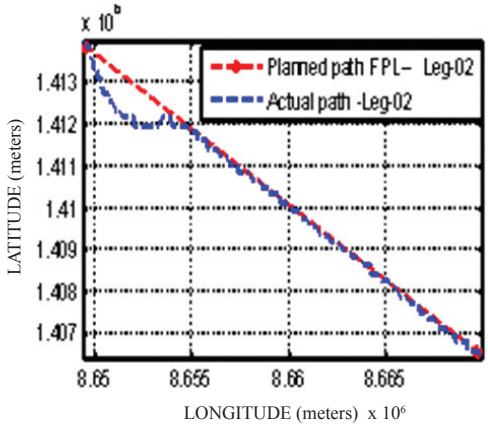

Figure 4. Navigation profile for leg-02.

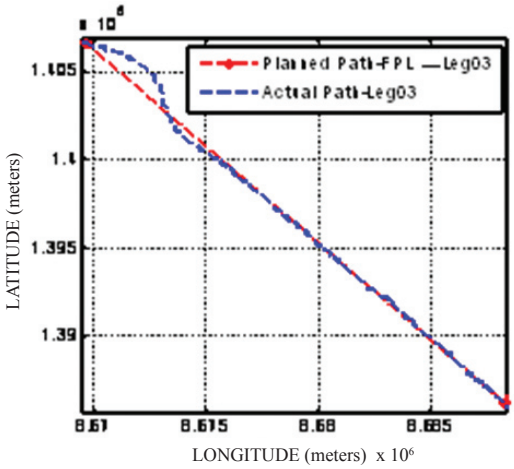

Figure 5. Navigation profile for Leg-03.

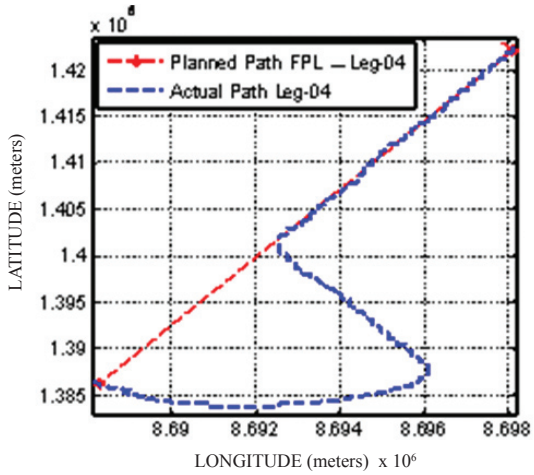

Figure 6. Navigation profile for leg-04.

the guidance mode remains the same till the last destination of the FPL is reached. The FPL destination index increments automatically while along-track component of the range is less than zero.

The Fig. 7 shows the switchover from DTF to CTF mode for leg-01 of the FPL, while the steering error is less than 5 deg.

The snapshots of the guidance cues on HUD in DTF and CTF modes are shown in Fig. 8 and Fig. 9 respectively.

In the DTF mode shown in Fig. 8, $\chi_{D} = \chi_{H = 150°}$, and $\chi_{= 156°}$. The steering error shown is, $\chi_{D} - \chi_{= -6°}$. Hence, the steering index is to the LH side. Under the CTF mode, the planned bearing of the leg shown in Fig. 9 is 126.5° and $\chi_{= 126°}$. Hence, the steering error is 0.5°. The steering cues on HUD in CTF mode point to the desired track rather than pointing directly to the destination.

The close navigation performance is evaluated at two stages,

(a) Comparing 'close nav cross' cue on HUD with respect to the target;

(b) Computing azimuth and depression co-ordinates of the symbol based on flight test data and comparing it with the pilot cue on HUD.

Initially, only baro ranging was implemented and this led to incorrect cue for the cases where height above destination

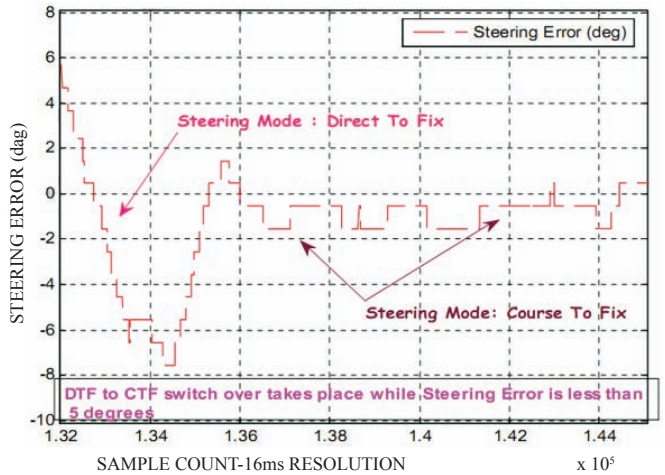

Figure 7. Leg 01- switchover from DTF to CTF mode.

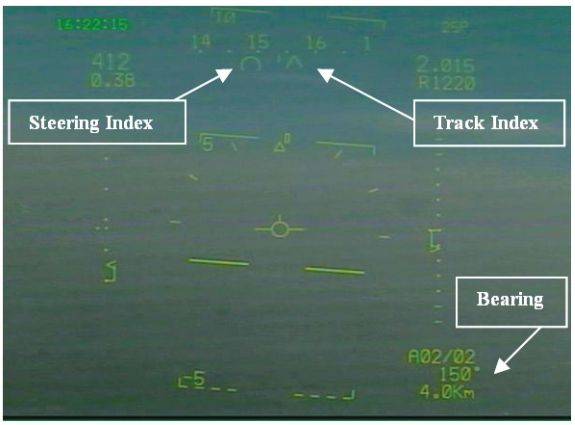

Figure 8. Guidance cues on HUD in DTF mode.

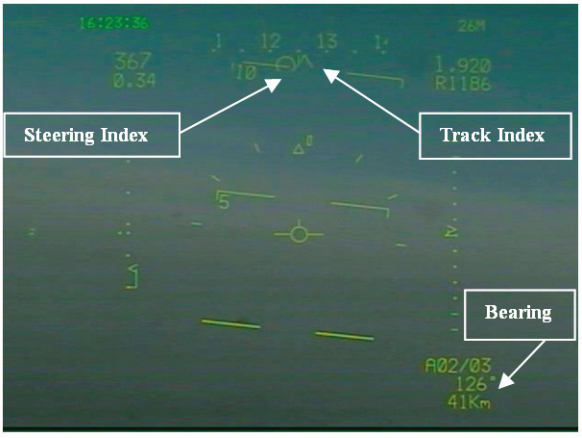

Figure 9. Guidance cues on HUD in CTF mode.

was invalid. Hence, the MC software was modified to take radio ranging as the next preferred ranging mode. Simulation studies were performed with radio ranging and with baro ranging under accurate H_D (height above destination) and found that the 'close nav cross' co-ordinates are giving correct cue to the target. If H_D is not entered and the radio height is also invalid, H_D is taken as zero for computing the 'close nav cross' co-ordinates. The close navigation co-ordinates for leg-01 have been shown in Fig 10.

The maximum cross track deviations ('*d*') during leg-02, leg-03 and leg-05 are within 1200 m. During leg-03,

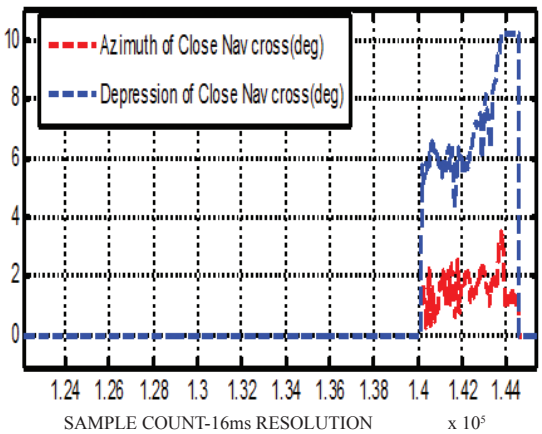

Figure 10. Leg 01- Close nav cross co-ordinates.

time taken to reach '*d*' near to zero from initial '*d*' of 1200 m is approximately 40 s (Ref: Fig 11). This performance was further improved by tuning the time constant't'. During leg-04 (Fig 12), the deviation has gone up to 7600 m which is mainly caused by the deviation in piloting with respect to the steering index (or steering pointer) and following bearing digits, just for cross checking the performance of steering index/pointer cue. The steering cues (including steering pointer/index, time to go, track index, drift angle, bearing, range, normalized time range circle, flight plan destination index and position cues) indications are tallying with the computed steering error as per guidance law.

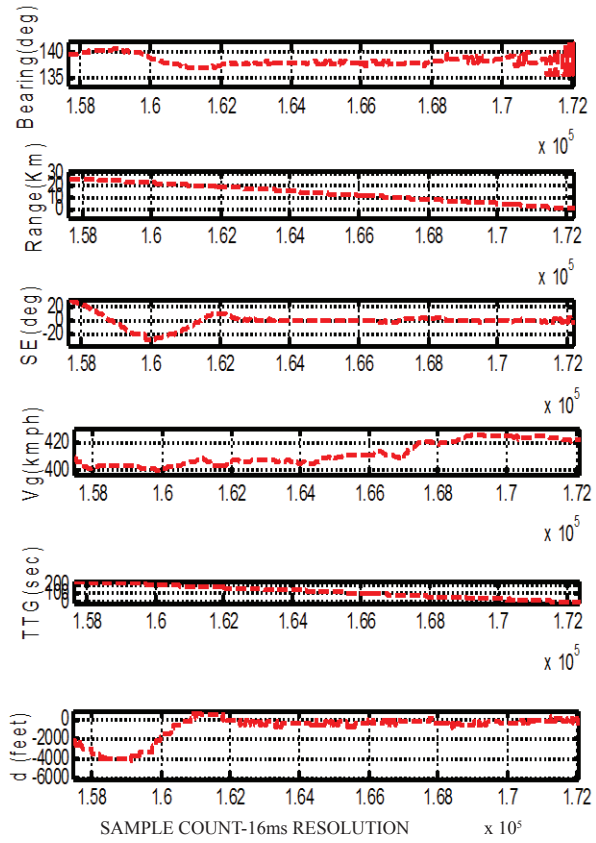

Figure 11. Analysis of leg 03.

The guidance law under FPL auto navigation was correctly leading to the planned track estimated to the destination under CTF guidance mode. The logic of switching from DTF to CTF in leg-01 also occurred as expected and thereafter the guidance mode remains to be in CTF till the end of auto navigation. The observation of large cross track deviation during the initial stage of the FPL leg was due to the piloting deviation with respect to the guidance cues on HUD. Another observation of incorrect 'close nav cross' cue at certain destination points was resolved by tweaking the algorithm for close navigation under baro ranging, radio ranging, and ranging for invalid destination height.

Case B: Manual Navigation

The manual FPL and waypoint navigation modes were performed during the flight after reaching DEST 06 and exiting from auto navigation mode. Orbits were performed under manual navigation mode and the performance guidance law in terms of steering cues was assessed. The guidance mode under manual navigation was initially DTF and then switched to CTF. The condition for DTF to CTF switching condition is either steering error less than 5° or 'time to go' is less than 10 s. If automatic leg switching is not selected, there is a requirement to steer back to a steer point after flying past it. The logic is implemented in the guidance law for switching back to DTF mode from CTF mode once the destination is crossed.

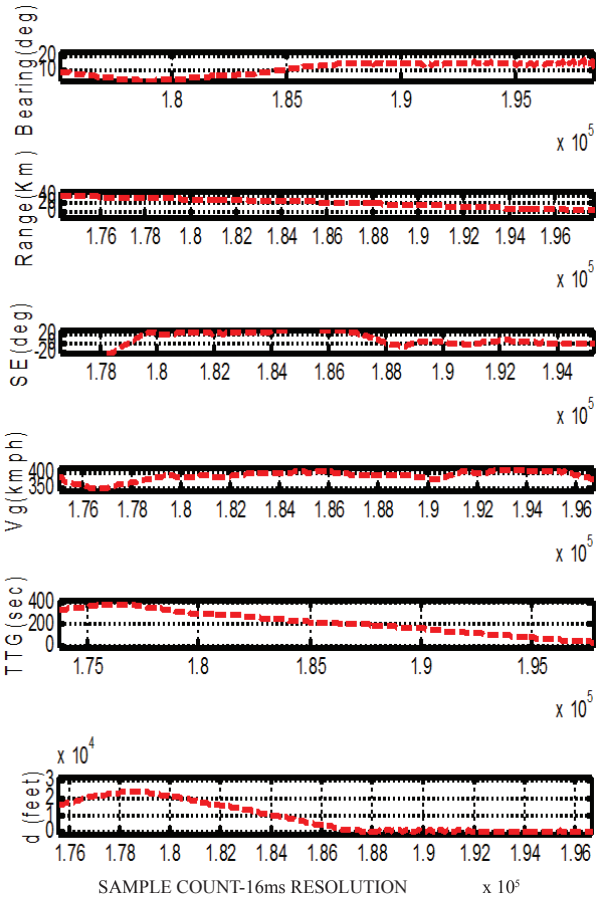

Figure 12. Analysis of Leg 04.

Case C: Dead Reckoned Mode

Under dead reckoned mode of navigation, GPS data is no longer valid. Hence, MC computes inertial velocity components based on true air speed components and previously computed wind velocity components. Fig. 13 indicates lateral guidance cues in DTF mode, under DR mode navigation. The MC computed inertial velocity components are shown in Figs. 14 and 15. Errors in this computations build up when the actual wind vector differs from MC estimated wind vector. The percentage of error in DR mode computation is shown in Table 3.

Under DR mode navigation, MC computes inertial velocity components V_n and V_e as follows,

$$V_n = V_{an} + W_n,$$
$$V_e = V_{ae} + W_e,$$

where,

$$V_{an}=V(L11\cos(\alpha)+N11\sin(\alpha)),$$
$$V_{ae}=V(L21\cos(\alpha)+N21\sin(\alpha)),$$

Figure 13. Manual WPT Navigation –DTF Mode.

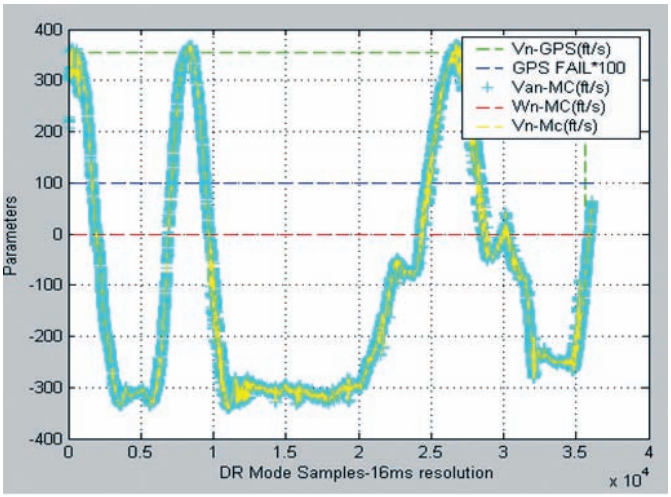

Figure 14. MC performance in DR mode, Velocity North computation.

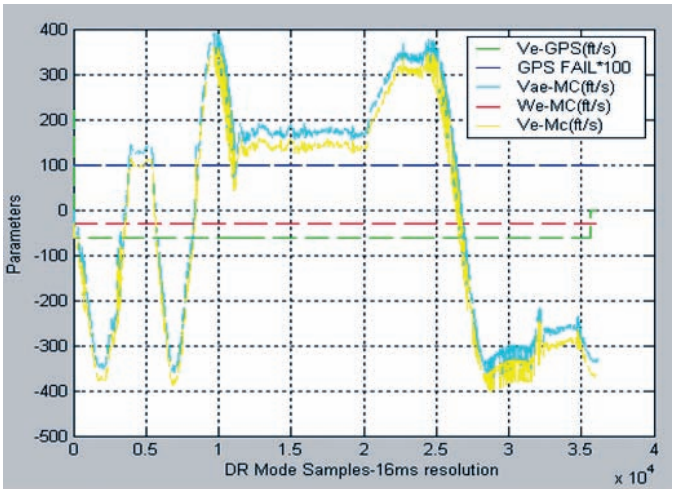

Figure 15. MC performance in DR mode, velocity east computation.

L11 = cos(θ)cos(Ψ),
L21 = cos(θ)sin(Ψ),
N11 = sin(θ)cos(φ)cos(Ψ)+ sin(φ)sin(Ψ),
N21 = sin(θ)cos(φ)sin(Ψ)-sin(φ)cos(Ψ),

here, W_n and W_e are east and north components of wind velocity used for navigation, and 'V' is true air speed.

Table 3. Error rate of MC computation under DR mode navigation

Avg. ground speed of aircraft (kmph)	Time (min)	Distance covered (m)	Error in MC – PP (m)	% Error
395	4.57	30162	1575.90	5.22
395	8.40	55440	2902.13	5.23

Case D: Position Error Estimation

The MC computed present position was compared with the DGPS, under valid GPS mode and DR mode. If valid GPS velocities are available, the computed inertial velocity components follow the GPS data. However, since the latter is only updated at 1 Hz, computed inertial velocity components are smoothened by complementary filtering with AHRS data.

It was observed that, the performance of the Navigation system under normal mode was limited by the low resolution of present position data updated by the GPS. The position error of 185.2 m can be caused just because of the poor resolution of GPS, which was 0.1 min. The Fig 16 shows the position cues from DGPS, GPS and MC processed for a different flight data. Later, the resolution of GPS was improved to resolution of 0.001 min (appx 1.852 m) and accuracy of 10 m.

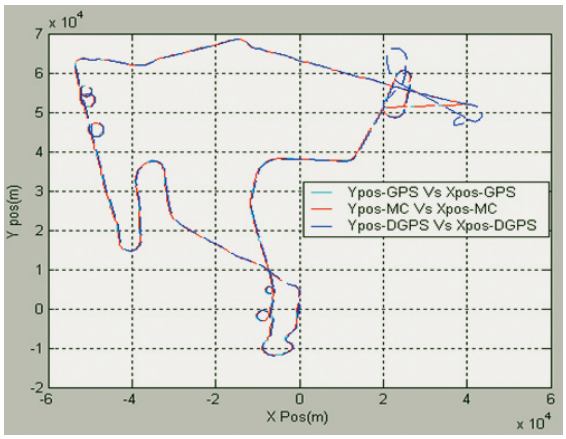

Figure 16. Position cue comparison.

Case E: Time Navigation Mode

Qualitative assessment of time navigation was made by creating a flight plan and by entering the expected time required to reach the destination, for each leg. The desired calibrated air speed to reach the destination at the specified time is computed as,

$$(V_c)_D = V_c + (V_D - V_g)\sqrt{\sigma}\ ,$$

where,

$(V_c)_D$ = Demanded CAS
V_c = Calibrated air speed

V_g = Ground speed
V_D = Demanded ground speed
σ = Air density ratio

The demanded speed is frozen for short ranges to destination or small differences between current and planned arrival times, to avoid the singularities or instabilities that would occur in such circumstances. The delay time entered by the test pilot is added to, or subtracted from the waypoint/destination time and used to adjust the time navigation calculations.

Case F: Radio Height Assessment

An innovative way of radio height assessment was carried out to validate the performance of onboard RADALT and performance of MC in processing radio height. The runway height (with reference to latitude) was first mapped using DGPS data. This was done during a low speed taxiing across the runway. The radio height processed by MC based on the RADALT sensor data was also recorded along with DGPS data and an additional onboard GPS data. Subsequently, aircraft was flown at different low altitudes above the runway (keeping latitude as the reference) and the RADALT altitude was compared with DGPS altitude corrected for runway height with reference to latitude. The Figs. 17 to 19 show the RADALT performance comparison with DGPS and additional GPS altitude (corrected for runway height) for radio height within 100 m, radio height 150-200 m range, and radio height about 1000 m respectively.

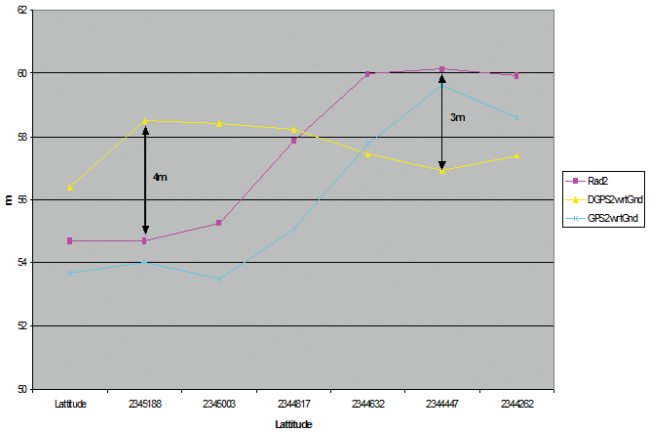

Figure 17. Radio height assessment – plot 1.

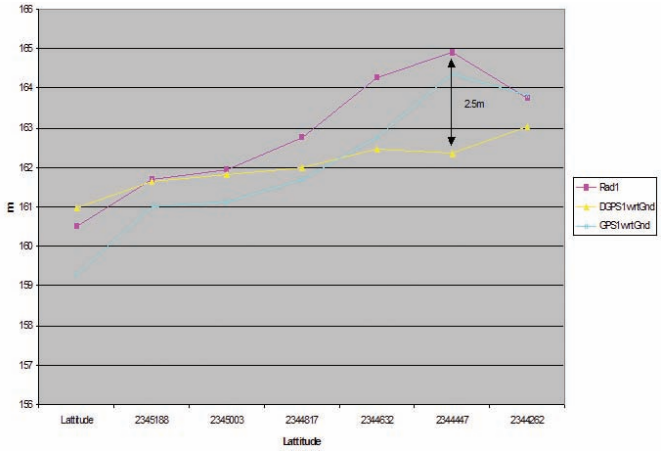

Figure 18. Radio height assessment–plot 2.

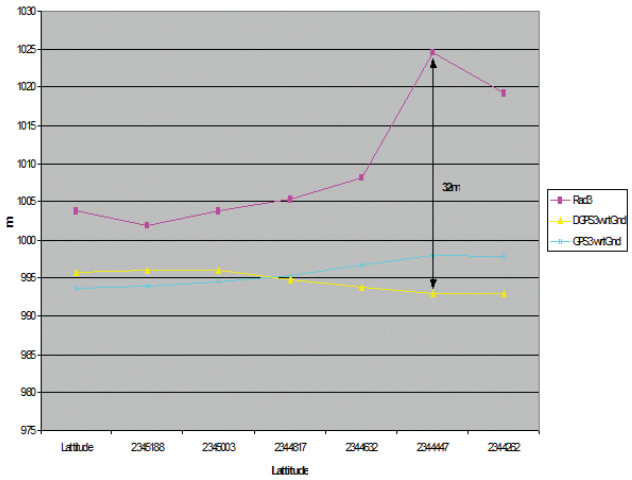

Figure 19. Radio height assessment–plot 3.

4. ASSESSMENT OF WEAPON AIMING ALGORITHMS

In-flight simulations of the weapon aiming modes were carried out. The MC generated weapon aiming displays in Air-To-Air (AA) and Air-To-Ground (AG) modes were assessed.

Case A: Air-to-Ground Ranging

The ranging modes include Radalt, Baro, and Fixed ranging modes. The actual ranging will be based on the validity of required parameter and the pre-defined sequence. If radio height becomes invalid under radio ranging mode, the integrated vertical velocity mode is used for limited time period. If valid ranging information is available, actual ranging mode is set to preferred ranging mode. Otherwise, next sensor in order of priority is determined. Under air to ground ranging, weapon aiming simulations were carried out for the modes like fixed mode, gyro stabilised mode, and CCIP mode. The snapshots of the HUD pages for these modes are shown in Figs. 19 to 21.

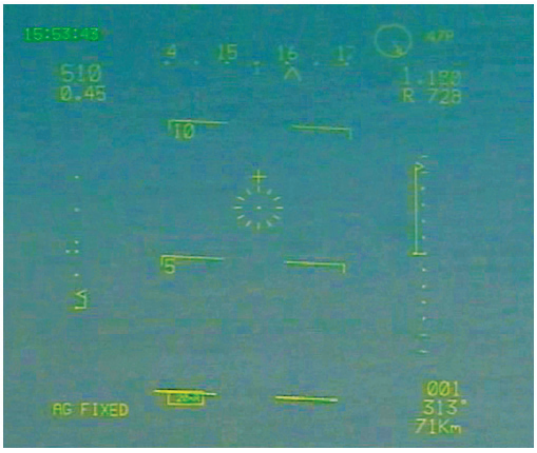

Figure 19. Air-to-ground fixed mode.

Case B: Air-to-Air Ranging

Under air-to-air ranging, weapon aiming simulation was carried out for the modes like lead angle computation (LAC) mode and continuously computed impact line (CCIL) mode.

The MC performs air to air gunnery computation based on

Figure 20. Air-to-ground gyro mode.

Figure 21. Air-to-ground CCIP mode.

lead angle computation (LAC). In LAC mode, user can set the target wing span and range. In the CCIL mode, MC calculates the initial shell velocity from the true air speed and angle of attack, and calculates a system state matrix used in calculating the co-ordinates of CCIL dots. Fig. 22 shows the HUD display under air to air CCIL mode.

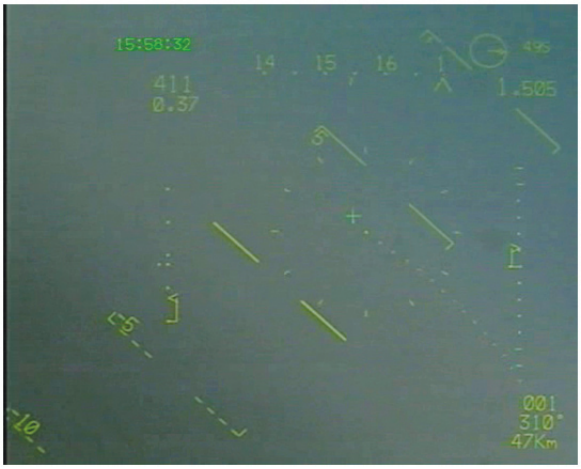

Figure 22. Air-to-air CCIL mode.

5. CHALLENGES AND INNOVATIONS

It was required to realize a low cost avionics suite with most of the subsystems are commercial off-the shelf items to reduce the development time. Instead of expensive inertial navigation system onboard, a mission computer with extensive data fusion of input data from relatively less expensive subsystems like GPS, AHRS, and ADS was considered. Apart from the sensor data fusion and other data processing, MC will be driving cockpit displays. The GPS refresh rate is limited to 1 Hz; the AHRS accelerations are quite noisy, and it doesn't provide velocity components or position coordinates at the output data stream. The AHRS acceleration parameters are available only in body axis. Also, the data from AOA vane and RADALT, and vertical velocity from ADC are also significantly noisy. The digital filtering of all these noisy data balancing the accuracy, response time, and stability; the appropriate complementary filtering cases to fuse the various parameters to derive the data set similar to the case of having INS was really a challenging task. Moreover, achieving the navigation accuracy of the order of 10 meters, proper smoothening of the navigation and guidance parameters by MC, reasonable accuracy for wind vector modelling and dead reckoned mode navigation, and smooth variation of parameters during dead reckoned mode to GPS valid mode transition were algorithmic intensive and innovative.

The flight testing of such algorithmic intensive system is also a complex task. The flight test plan and schedule was vetted with many considerations which include the provision of DGPS for reference checks, surveying of the target location, user way point database generation, loading of the mission data in to GPS and MC, synchronization of data and video recorded at different systems, offline simulation studies, and flight profile recreation. The wind vector estimation by MC was validated using the ground speed and true air speed. Also, the wind vector estimated by MC during take-off roll was compared with the air traffic control reported wind velocity. The dead reckoned mode was initiated by switching off GPS and then continued the flying at the same altitude and heading. This flying scenario was adopted to ensure the correctness of wind vector assumption for dead reckoned navigation. Innovative method was also adopted for radio height validation by mapping the runway terrain using DGPS using latitude as the reference and then flying at different low altitudes.

6. CONCLUSIONS

Flight evaluation of mission computer algorithm is carried out by assessing its performance under various navigation and guidance modes. Performance analysis of the flight test data and simulation results under different navigation modes suggest that the onboard guidance law has reasonably good tracking performance under manual and auto navigation modes. Performance under dead reckoned, close navigation, and time navigation modes are addressed in this paper. In-flight simulation of the weapon aiming modes has also been addressed in the paper. The challenges and innovations involved are discussed in the paper. In future, the amount of flight testing efforts can be considerably reduced with the utilization of extensive mission simulators and stimulators from the initial stage of the aircraft development programme itself.

7. ACKNOWLEDGMENTS

We express our sincere thanks to the Chief Test Pilot and the members of flight operations team at Hindustan Aeronautics Limited (HAL) Bangalore, who took lead in scheduling, performing, real time monitoring and de-briefing of the test flights. We are thankful to the programme management, senior officers, and colleagues at Aircraft Research and Design Centre (ARDC), HAL for their encouragement and support.

REFERENCES

1. Rajesh, A.K.; Saraswathi, Nagarajan C. & Prasad, H.R.S. Flight test evaluation of guidance algorithm for a modern trainer. *In* the 47th Israel Annual Conference on Aerospace Science, 21st-22nd Feb 2007, TelAviv and Haifa
2. Ching-Famg, Lin. Modern Navigation, guidance and control processing, Prentice Hall Inc., 1991.
3. Yechout, Thomas R.; Morris, Steven L.; Bossert, David E. & Hallgren, Wayne F. Introduction to aircraft flight mechanics: Performance, static stability, dynamic stability, and classical feedback control. *In* AIAA Education Series, TL671.4.T43. AIAA, 2003.

Contributors

Ms Gargi Meharu received her BE (Electr. Comm. Eng.) and joined HAL in 2005. Currently, she is pursuing MS(Aerospace Vehicle Design) at Cranfield University, UK. She is working as Deputy Manager (Design-Avionics) at Aircraft Research & Design Centre (ARDC), Hindustan Aeronautics Ltd (HAL). Her interest areas include : Avionics system design & development, system integration, flight test evaluation, and data analysis.

Mr Sunil K. Valsan received his BTech (Electr. Comm. Eng.) from Kerala University and joined HAL in 2002. He is working as Manager (Design-Avionics) at ARDC, HAL. His iinterest areas include : Avionics system design & development, system integration, development of integration rigs, flight test evaluation, and data analysis.

Dr Rajesh A. Kuttieri obtained his MS (Software Systems) from BITS, Pilani and PhD (Aerospace Engineering) from IIT, Kharagpur. He is working as Senior Manager (Design-Avionics) at ARDC, HAL. His interests include : Avionics system design, development and certification, aircraft parameter estimation, artificial intelligence, adaptive flight control system, aerospace vehicle design, etc.